Accepted Manuscript

Design, synthesis and biological assessment of *N*-adamantyl, substituted adamantyl and noradamantyl phthalimidines for nitrite, TNF-α and angiogenesis inhibitory activities

Weiming Luo, David Tweedie, Shaunna L. Beedie, Neil Vargesson, William D. Figg, Nigel H. Greig, Michael T. Scerba
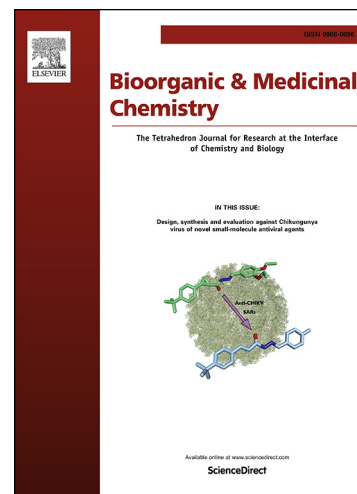
Please cite this article as: Luo, W., Tweedie, D., Beedie, S.L., Vargesson, N., Figg, W.D., Greig, N.H., Scerba, M.T., Design, synthesis and biological assessment of *N*-adamantyl, substituted adamantyl and noradamantyl phthalimidines for nitrite, TNF-α and angiogenesis inhibitory activities, *Bioorganic & Medicinal Chemistry* (2018), doi: https://doi.org/10.1016/j.bmc.2018.01.032

Design, synthesis and biological assessment of *N*-adamantyl, substituted adamantyl and noradamantyl phthalimidines for nitrite, TNF-α and angiogenesis inhibitory activities

Weiming Luo[a], David Tweedie[a], Shaunna L. Beedie[b,c], Neil Vargesson[b], William D. Figg[c], Nigel H. Greig[a*], Michael T. Scerba[a]

[a] Drug Design & Development Section, Translational Gerontology Branch, Intramural Research Program, National Institute on Aging, National Institutes of Health, Baltimore, MD 21224, USA

[b] School of Medicine, Medical Sciences and Nutrition, Institute of Medical Sciences, University of Aberdeen, Foresterhill, Abrerdeen, AB25 2ZD, UK

[c] Molecular Pharmacology Section, National Cancer Institute, National Institutes of Health, Bethesda, MD 20892, USA

*corresponding author: Nigel H Greig, greign@grc.nia.nih.gov 251 Bayview Blvd, BRC Room 05C220, Baltimore MD 21224

Abstract

A library of 15 novel and heretofore uncharacterized adamantyl and noradamantyl phthalimidines was synthesized and evaluated for neuroprotective and anti-angiogenic properties. Phthalimidine treatment in LPS-challenged cells effected reductions in levels of secreted TNF-α and nitrite relative to basal amounts. The primary SAR suggests nitration of adamantyl phthalimidines has marginal effect on TNF- αactivity but promotes anti-nitrite activity; thioamide congeners retain anti-nitrite activity but are less effective reducing TNF-α. Site-specific nitration and thioamidation provided phthalimidine **24**, effecting an 88.5% drop in nitrite concurrent with only a 4% drop in TNF-α. Notable anti-angiogenesis activity was observed for **20**, **21** and **22**.

1. Introduction

Neurons are highly specialized cells that comprise the central nervous system and interact through a series of complex chemical and voltage-dependent signaling motifs. Like all cells, neurons maintain homeostasis through carefully regulated processes that identify and subsequently respond to physiological strains including high biosynthetic or secretory demands, changes in oxidative/nitrosative[1] redox balance, inflammation and aging. In this regard, healthy neurons are typically able to endure episodes of short, intense trauma in addition to periods of lingering, mild stress. However, in the case of vulnerable neurons, the magnitude of such circumstances can promote synapse loss, pruning, cellular dysfunction and even death.[2] Depending on the neuronal population or brain region involved, these actions may lead to neurodegenerative disorders such as Alzheimer's disease (AD), Huntington's disease (HD), Parkinson's disease (PD) and multiple sclerosis (MS).[3]

Specific families of proteins, small molecules and biochemical signal-transduction pathways orchestrate these events. For instance, the pro-inflammatory release of tumor necrosis factor-alpha (TNF-α) by microglia can initiate damaging, self-propagating cycles of inflammation if not appropriately regulated in a time-dependent manner.[4] TNF-αlevels are found consistently elevated by as much as 25-fold in the cerebrospinal fluid (CSF) of AD patients.[5] In addition, subjects with mild cognitive impairment that progress to develop AD suggest that increased CSF TNF-αlevels are an early event, and their rise correlates with disease progression.[6] In a similar fashion, an upsurge of nitric oxide (•NO, **Figure 1**)[7] produced by neuronal nitric oxide synthase (nNOS) or inducible nitric oxide synthase (iNOS) in response to traumatic insult and chronic inflammation is perhaps one of the key midstream elements in the evolution of AD, MS and PD.[8] For instance, amyloid-β 1-40 peptide ($A\beta_{1-40}$) challenge was sufficient to induce a 50-fold profusion of NOS-derived nitric oxide in microglial cells as compared to basal amounts, while simultaneous administration of $A\beta_{1-40}$ and pro-inflammatory interferon-γ effected an even greater 100-fold release.[9] Overproduction of NO has also been associated with increased angiogenesis in

tumor lines, leading to expanded vascularization and the progression of certain types of cancer. The mass, degree of vascularization and growth rate of tumors induced by iNOS-clone cell treatment in a population of CD1 *nu/nu* mice was directly related to NOS-produced NO; combined nitrite/nitrate levels observed in iNOS clones were roughly 70-fold higher at one week relative to wild-type cells, while the resulting tumors in the treated mice were three times heavier at one month and possessed 5-fold more vasculature. [10]
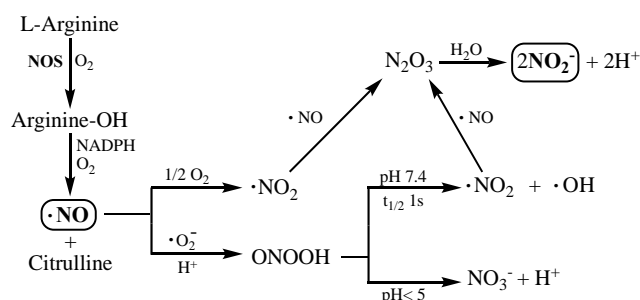

Figure 1. Nitric oxide synthase (NOS) catalyzed production of NO and subsequent conversion of ROS (reactive oxygen species) and RNS (reactive nitrogen species) to nitrite in *vivo*.

Our recent interests on thalidomide analogs effecting anti-inflammatory responses[11] led us to investigate new congeners for desirable neuroprotective properties. To our surprise, a detailed chemical and biological evaluation of substituted *N*-adamantyl phthalimidines was lacking in the literature. It has been shown that strategic incorporation of adamantyl groups can impart numerous benefits to neuroprotective and anti-inflammatory agents (**Figure 2**).[12] The unique hydrophobic structure bestows increased lipophilicity, facilitating traverse across biological membranes such as the blood-brain barrier. In addition, the large rigid, cage-like skeleton often prevents excessive catabolism and can strengthen desirable interactions with CNS targets. For instance, amantadine **1** and memantine **2** have shown promise for the treatment of AD and PD, functioning as *N*-methyl-D-aspartate receptor antagonists and also by reducing microglia-associated inflammation.[13] The specific size and hydrophobicity imparted by the adamantyl groups are among the key factors in determining the affinity and activity of these ligands. Given the scope of inflammation-associated neurodegenerative disorders coupled with their complicated and potentially intertwined mechanisms of incipience, we set out to develop a series of new chemical entities featuring the substituted *N*-adamantyl motif and possessing desirable neuroprotective properties. Herein we report the design, synthesis and evaluation of 15 novel and heretofore uncharacterized substituted adamantyl and noradamantyl phthalimidines with nitrite, TNF-αand angiogenesis inhibitory activities.
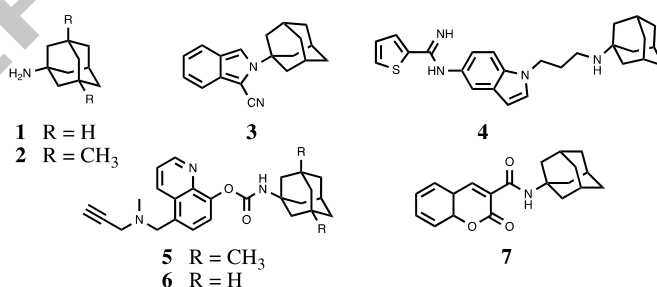

Figure 2. Neuroprotective agents containing the adamantyl moiety

## 2. Results and Discussion

2.1 Synthetic chemistry

We constructed our phthalimidines with two key pharmacophores in mind. Initially intrigued by thalidomide analogs with known anti-inflammatory activities,[14] we envisioned each of our new molecules would feature an aromatic isoindolinone framework. Upon these scaffolds, we would install appropriate adamantyl or noradamantyl moieties, ultimately yielding our family of *N*-substituted phthalimidines. For compounds **9-13**, we utilized a simple one-pot approach. Phthaldialdehyde **8** was combined with various adamantyl or noradamantyl amines to produce the desired products in acceptable yields (**Scheme 1**). The proposed mechanism of formation is not clear, but is believed to involve a tandem iminium rearrangement and elimination or, alternatively, a [1-5]-H

sigmatropic shift.[15] Aryl-substituted phthalimidines **16-22** were prepared using a stepwise process (**Scheme 2**). Initially, methyl 2-methyl-3-nitrobenzoate **14** was subjected to benzylic radical bromination to generate intermediate **15**.[16] Subsequent condensation with the appropriate amines provided the desired nitrated products in satisfactory yields. Catalytic hydrogenation of **20** provided aniline **21**. Thioamides **23-25** were obtained from the corresponding parent isoindolinones by treatment with Lawesson's reagent (**Scheme 3**). A summary of novel phthalimidines is presented in **Figure 3**.
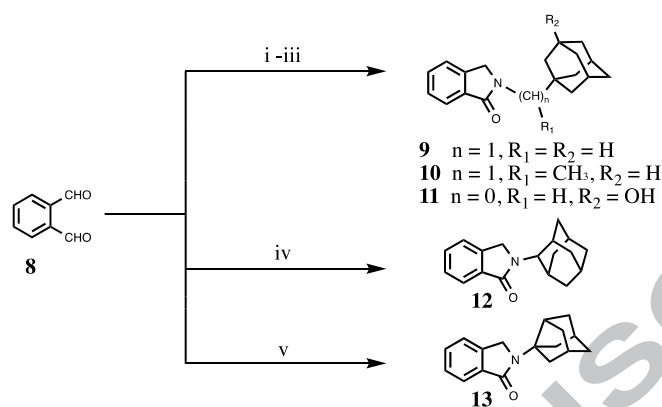
Scheme 1. Reagents and conditions: (i) 1-adamantanemethylamine (for **9**), THF; (ii) 1-(1-adamantyl)ethylamine hydrochloride (for **10**), K$_2$CO$_3$, THF; (iii) 3-amino-1-adamantanol (for **11**), THF; (iv) 2-adamantylamine hydrochloride (for **12**), K$_2$CO$_3$, THF; (v) 3-noradamantanamine hydrochloride (for **13**), K$_2$CO$_3$, THF.
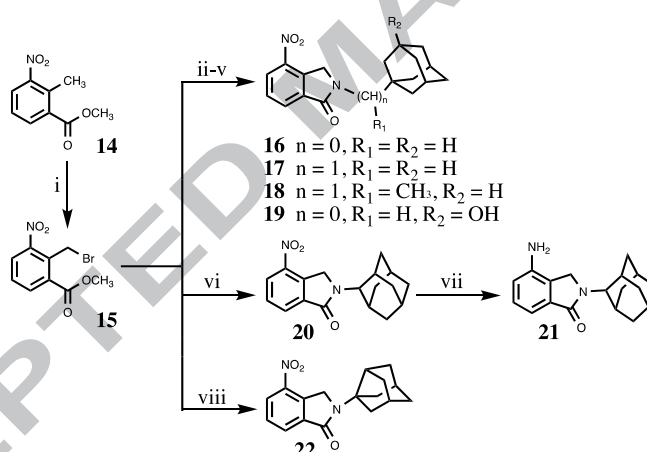
Scheme 2. Reagents and conditions: (i) NBS, benzoyl peroxide (for **15**), CCl$_4$, reflux; (ii) 1-adamantylamine (for **16**), K$_2$CO$_3$, DMA, rt to 50 °C; (iii) 1-adamantanemethylamine (for **17**), K$_2$CO$_3$, DMA, rt to 50 °C; (iv) 1-(1-adamantyl)ethylamine hydrochloride (for **18**), K$_2$CO$_3$, DMA, rt to 55 °C; (v) 3-amino-1-adamantanol (for **19**), K$_2$CO$_3$, DMA, rt to 58 °C; (vi) 2-adamantylamine hydrochloride (for **20**), K$_2$CO$_3$, DMA, rt to 58 °C; (vii) H$_2$, Pd-C(10%), MeOH, rt; (viii) 3-noradamantanamine hydrochloride (for **22**), K$_2$CO$_3$, DMA, rt to 50 °C.
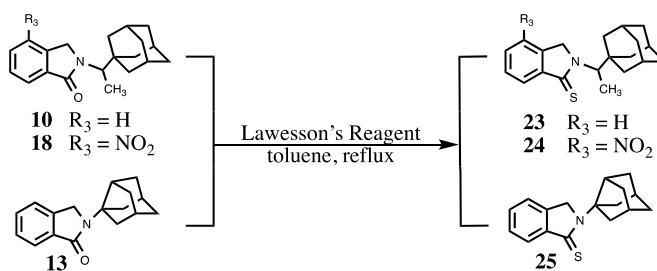
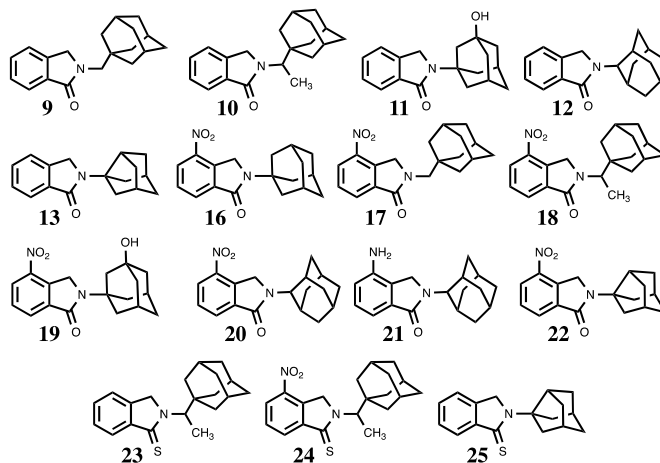**Scheme 3.** Synthesis of adamantyl phthalimidine thioamide congeners.

Figure 3. Structures of novel adamantyl and noradamantyl phthalimidines

2.2 NO$_2^-$ and TNF-α inhibitory activities

Once we had our phthalimidine library in hand, we set out to evaluate our molecules for anti-TNF-α and nitrite activities. Fortunately, the RAW 264.7 cellular model of inflammation identifying NO$_2^-$ and TNF-α inhibitors had been reported and was well established.[17] Inhibitory activities of LPS-induced NO$_2^-$ and TNF-α production in RAW 264.7 cells along with cell viability and computed lipophilicity (Clog D value) are shown in **Table 1**.[18] The data afforded some notable observations upon first inspection. We were pleased that our compounds were not appreciably cytotoxic, with most retaining >80% cell viability at 30µM treatment. It also appeared that polar compounds did not fare particularly well in either assay; even the leading –NH$_2$ and -OH substituted inhibitors reduced nitrite by only 28% (amino compound **21**) and TNF-α by 20% (hydroxy compound **11**). While a few compounds effected moderate reductions of both analytes, TNF-α inhibition was clearly less prominent overall. Foremost TNF-α inhibitor **13** reduced levels to only 52% of the control (vehicle treatment) value, whereas five phthalimidines diminished nitrite levels below 50%. We also noted that compounds with a Clog D value below 3.0 performed poorly in the nitrite assay, generally failing to curtail levels below 70%. Compound **22** was the sole exception, reducing nitrite to 49% concurrent with a Clog D of 2.79. Conversely, of the ten phthalimidines with Clog D values greater than 3.0, eight reduced nitrite amounts below 60%, and four of these further diminished levels well into the sub-50% range.

When the data was examined more prudently, we became aware of some specific trends in the primary structure-activity relationship. Analysis of a series of phthalimidine and thioamide counterparts revealed the parent amides as superior inhibitors of TNF-α production. On average, TNF-α levels were decreased to 72%, 55% and 52% with amide congeners **18**, **10**, and **13**, respectively (**Figure 4**, **plot a**). We did not observe any prominent link between thioamidation and nitrite activity. When we investigated the influence of aromatic nitration on TNF-α and nitrite activity, we noticed an interesting phenomenon. It was clear that unsubstituted hydro analogs were more effective regulators of TNF-α than their corresponding nitro derivatives. (**Figure 4, plot b**). For instance, in the case of the **22**/**13** grouping, nitrated **22** permitted 90% TNF-α secretion while hydro compound **13** effected 52% activity. However, when similar phthalimidine pairings were analyzed in the nitrite assay, we discovered an opposing trend. Nitration was clearly beneficial to anti-nitrite activity (**Figure 5a).** The effects were quite dramatic in **23**/**24** and **12**/**20** where nitrite levels were reduced, on average, from 52% to 11.5% and from 62% to 9.2%, respectively. It should be noted that in regards to 2-adamantyl substrates **12**, **20**, and **21,** the results appear specifically attributable to the nitro group, not manifest by simple or arbitrary substitution at the isoindolinone 4-position (**Figure 5b**.)

Table 1. Adamantyl-substituted phthalimidine inhibition of LPS-induced nitrite and TNF−α production in RAW 264.7 cells.

#[a]	Nitrite		TNF-α activity[d]		Cell Viability		Clog D
	%Δ[b]	P	%Δ[b]	P	%Δ[b]	P	
9	50±3	0.0079	59±8	0.0093	81±15	0.2225	3.72
10	52±4	0.0092	55±4	0.0026	82±3	0.0071	4.25
11	101±3.5	0.8674	80±2.3	0.0098	98±4.0	0.7527	1.87
12	62±10.6	0.0319	58±3.8	0.0029	75±4.2	0.0064	3.51
13	N/A[e]	N/A	52±3	0.0007	74±1	<0.0001	2.88
16[c]	40±4	0.0003	86±4	0.0467	114±9	0.2024	3.29
17	55±0.6	0.0015	77±2.0	0.4152	92±0.8	0.0149	3.63
18	35±3.9	0.0002	72±8.3	0.0857	81±3.8	0.0105	4.16
19	94±1.2	0.5117	91±2.3	0.0953	107±3.9	0.1557	1.78
20	9.2±1.3	<0.0001	65±2.1	0.0004	82±3.3	0.0074	3.42
21	72±3.4	0.0018	101±9.2	0.8952	99±2.8	0.9435	2.49
22	49±1.1	0.0068	90±1.3	0.1080	92±2.2	0.0734	2.79
23[c]	52±4	0.0092	90±6	0.1662	84±2	0.0820	4.67
24	11.5±0.3	0.0083	96±1.2	0.3553	83±1.9	0.0013	4.58
25[c]	N/A[e]	N/A	85±4	0.0301	94±5	0.4769	3.30

Values presented in the table are mean ± S.E.M. of n=3 measurements. A Student's t test was used to asses for statistically significant changes; P<0.05 was considered significant. Clog D are calculated log D values determined at pH 7.0 (CompuDrug, Pallas).
[a] compounds screened at 30μM for nitrite, TNF-α, and viability assays
[b] percentage of vehicle control value; vehicle control = 100% analyte
[c] compounds were not completely soluble at 30μM; **16, 23** and **25** were partially precipitated upon addition to the cell culture media
[d] For comparison, the known TNF-α inhibitor Lenalidomide effects TNF activity of 109% ± 10 with P = 0.4482 (see reference 18 for further detail)
[e] Data was not available as the levels in the control media (i.e. DMSO + LPS) were lower than the lowest level on the nitrite values on the standard curve.
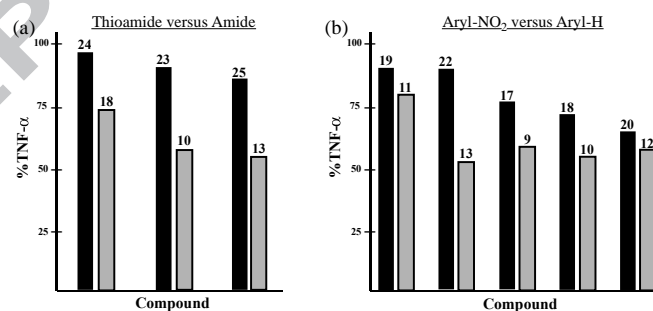

Figure 4. Effects of thioamidiation and aromatic nitration in strucurally related adamantyl phthalimidines on levels of secreted TNF-α. The compounds listed in each bar pair differ only at the site of indicated subsitution. Data extrapolated from **Table 1** and presented graphically as the mean % change of TNF-α activity relative to the control. (a) Comparison of thioamide (C=S) and amide (C=O) congeners on levels of secreted TNF-α. Thioamides are shown as the left bar of each pair; their corresponding amides appear on the right. (b) Comparison of 4-nitro (-NO$_2$) and 4-hydro (-H) substituted congeners on levels of secreted TNF-α. Phthalimidines with 4-nitro-substituted isoindolinone cores are depicted as the left bar of each pair; their corresponding unsubstituted 4-hydro version appears on the right.
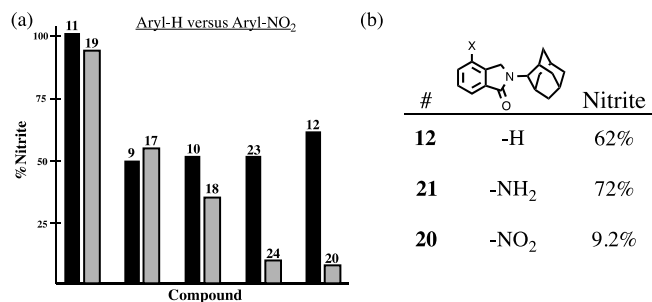
Figure 5. Effects of aromatic nitration on nitrite production. Data extrapolated from **Table 1** and presented as the mean % change of nitrite activity relative to the control. (a) The compounds listed in each pairing differ only by the presence/absence of a nitro group in the isoindolinone 4-position. Hydro versions appear on the left, while nitro analogs appear on the right. (b) Comparison of 4-position substituent effects.

We also noticed that within groups of structurally related phthalimidines, increasing *N*-substituent bulk typically resulted in evolution or enhancement of anti-nitrite activity. Taking the form of methyl additions or noradamantyl ring expansions, these steric progressions are clearly reflected in the associated Clog D values (**Figure 6**). For example, in the case of the simple phthalimidines from Group A, noradamantyl **13** possessed a Clog D of 2.88 and effected no detectable change in nitrite while the larger adamantyl **12** registered a modest 62% reading along with a Clog D of 3.51. In the case of groups B and C, it was clear that methylation was well tolerated. While, admittedly, the performance of **9** was not improved significantly upon methylation to **10,** it is important to stress that the activity was not compromised. It was quite apparent, however, that methylation enhanced the anti-nitrite activity of **17**. While average nitrite was reduced to 55% of control amounts with des-methyl **17,** production was curtailed to 35% with corresponding methylated analog **18**. Finally, the pattern seen in nitro-substituted compounds from Group D was particularly noteworthy, with ring expansion from noradamantyl **22** to adamantyl entries **16** and **20** having the marked effect of increasing steric bulk and Clog D concurrent with decreasing average nitrite levels from 49% to 40% and 9.2%. Fortunately, these findings parallel and expand upon our earlier premise relating heightened Clog D and general nitrite inhibition.

When considering these observations within the context of the data as a whole, perhaps the most salient finding is that compound **24** effects significant nitrite inhibition but leaves TNF-α essentially unperturbed. Analyzed in the logical progression, a focused series of phthalimidines correlates this selective anti-nitrite activity with consolidation of steric bulk, nitration and thioamidation (**Table 2**). The least-encumbered substrates **25** and **13** effected no detectable change in nitrite levels but clearly illustrated that thioamidation enhanced relative TNF-α production. As the bulk surrounding the phthalimidine nitrogen was progressively increased from noradamantyl in **13** to 2-adamantyl in **12** through alkyl-adamantyl in **10**, TNF-α remained approximately 50% of control amounts, while nitrite levels began to decrease steadily. Des-methyl analog **17** reaffirmed that aromatic nitration enhances anti-nitrite activity, notwithstanding the slight decrease in steric bulk. Upon reintroduction of the methyl group in **18**, TNF-α levels remained elevated but nitrite levels expectedly diminished in accordance with the increased lipophilicity. Ultimately, when appropriate sterics, nitration and thioamidation were united in **24**, nitrite levels plummeted to 11.5% while TNF-α remained at 96% of the control, notably suggesting that **24** functions as a selective nitrite inhibitor under our assay conditions. This evolution of selective anti-nitrite activity is further illustrated and summarized in **Figure 7**. As the progression of compounds unfolds from **25** to **24**, the Clog D (represented by the left axis and corresponding to the grey bars) trends upwards. As these values increase, an inflection is reached at compound **10**. After this point, the associated analyte levels begin to differentiate and diverge. Quantified by the right axis, TNF-α (*) begins to rise while nitrite (●) begins to fall. When **24** is reached, Clog D is at its pinnacle, TNF-α remains high, and nitrite is substantially reduced.

Group	Compound	Structure	Formula	CLogD	% Nitrite
A	13		$C_{17}H_{19}NO$	2.88	N/A
	12		$C_{18}H_{21}NO$	3.51	62
B	9		$C_{19}H_{23}NO$	3.72	50
	10		$C_{20}H_{25}NO$	4.25	52
C	17		$C_{19}H_{22}N_2O_3$	3.63	55
	18		$C_{20}H_{24}N_2O_3$	4.16	35
D	22		$C_{17}H_{18}N_2O_3$	2.79	49
	16		$C_{18}H_{20}N_2O_3$	3.29	40
	20		$C_{18}H_{20}N_2O_3$	3.42	9.2

Figure 6. Effects of relative *N*-substituent bulk in strucurally related phthalimidines on levels of secreted nitrite. The progression of structures in each group reflects the net addition of CH_2 to the initial compound. Data absorbed from **Table 1** and presented as the mean % change of nitrite activity relative to the control.

Table 2. Structure-activity trends in a family of substituted phthalimidines.

compound	structure	Clog D	% TNF-α[a]	% nitrite[a]
25		3.30	85	N/A[b]
13		2.88	52	N/A[b]
12		3.51	58	62
10		4.25	55	52
17		3.63	77	55
18		4.16	72	35
24		4.58	96	11.5

[a] Analyte % are represented as average % of analyte relative to control samples. Raw data absorbed from **Table 1**.
[b] Data was not available as the levels in the control media (i.e. DMSO + LPS) were lower than the lowest level on the nitrite values on the standard curve.
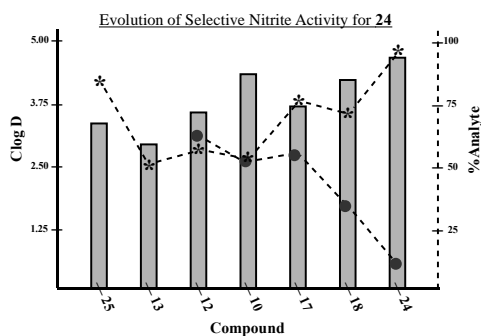
Evolution of Selective Nitrite Activity for **24**

Figure 7. Graphical summary of selective anti-nitrite activity for compound **24**. The focused library of phthalimidines is listed on the X-axis in progression towards compound **24**. The corresponding grey bars represent Clog D values and are plotted via the left axis. The assocaited nitrite (●) and TNF-α (∗) percentages are plotted via the right axis. Data extrapolated from **Table 1** and presented graphically as the mean % change of analyte relative to control values.
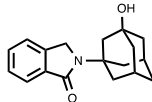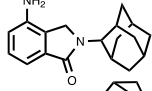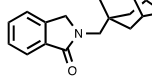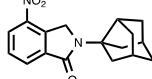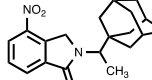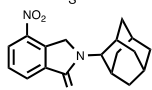
2.3 Anti-angiogenesis activity

Given the anti-nitrite characteristics of our novel phthalimidines, we wondered what effect our molecules would have on angiogenesis in a model system. We took advantage of the *fli1*:EGFP zebrafish embryo model for determining *in vivo* angiogenic responses.[19] In short, embryos were developed for 24 hours and then exposed to the phthalimidines of interest. During this period, the vasculature grows rapidly, producing new intersegmental vessels (ISVs). After an additional 24 hours of phthalimidine incubation, the zebrafish embryos were anaesthetized and analyzed for phthalimidine-sensitive angiogenic behavior. When compared to the control (vehicle alone) system, anti-angiogenic activity was evidenced by loss of ISVs or relative decreases in ISV outgrowth.

For this preliminary evaluation, we opted for a condensed series of phthalimidines spanning the range of anti-nitrite activity. We chose molecules affording an extensive selection of functional groups and skeletal backbones while also considering the logical progression and evolution of the anti-nitrite structure-activity relationship (**Table 3**). Compounds were initially tested at a low dose of 10μg/mL, roughly on par with the 30μM concentrations utilized in the preliminary TNF-α/nitrite screen. At first glance, the data appears quite erratic without any particular trends. When vessel length and vessel number are plotted according to increasing anti-nitrite ability, both parameters seem to fluctuate sporadically (**Figure 8**). However, an interesting pattern emerges when the combined data is plotted against Clog D (**Figure 9**). Based upon this focused series of phthalimidines, it appears that compounds at the extremes of Clog D behave unfavorably and in some cases, promote angiogenesis relative to the control. However, there does appear to be an anti-angiogenic sweet-spot localized around Clog D ≈ 2.8, where both vessel length and vessel number converge toward a minimum. In this regard, compound **22** was clearly the most effective molecule studied in this preliminary screen. Interestingly, the selective nitrite efficacy of **24** did not translate into notable anti-angiogenic activity in the zebrafish assay. On the contrary - compound **24** proved no more effective than the vehicle at decreasing vessel length and moderately bolstered vessel number relative to vehicle.

We selected compounds **20**, **21**, and **22** as the most promising anti-angiogenic candidates and subsequently analyzed each at increasing concentrations for evidence of dose-response behavior. Compound **20** appeared quite toxic, proving lethal to zebrafish at concentrations above 5μg/mL. Phthalimidines **21** and **22** were more well behaved, demonstrating dose-dependent decreases on vessel length for concentrations up to 50μg/mL (Figure **10**). However, beyond this threshold the compounds became exceedingly toxic to zebrafish and we therefore chose to conclude our preliminary screen.

Table 3. Anti-angiogenesis properties of substituted phthalimidines.

compound	structure	% nitrite[a]	vessel length[b]	# of vessels[c]
11		101	105.1±4.9	19.5±0.5
21		72	42.1±3.3	14.0±1.4
9		50	83.1±2.4	18.2±0.4
22		49	42.8±9.2	8.6±2.7
24		11.5	86.4±2.8	22.0±0.5
20		9.2	48.2±1.9[d]	14.6±0.6[d]

[a]nitrite data extrapolated from **Table 1**; presented as mean % of control
[b]vessel length in μm, obtained at 10μg/mL; presented as mean ± S.E.M
[c]vessel number obtained at 10μg/mL; values presented as mean ± S.E.M
[d]compound **20** screened at 5μg/mL; values presented as mean ± S.E.M

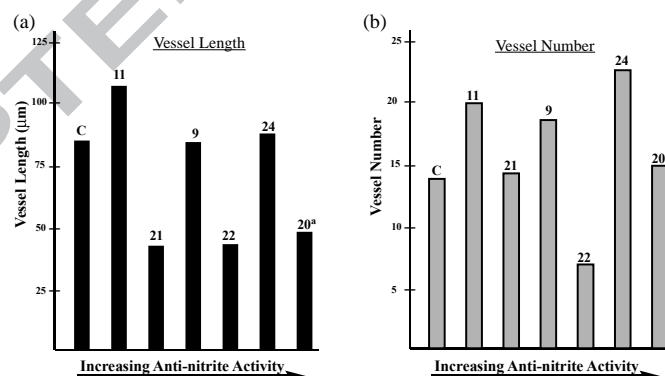**Figure 8.** Summary of anti-angiogeneis data for a focused family of adamantyl phthalimidines. Data obtained at 10μg/mL dosage. Each bar corresponds to an indicated novel phthalimidine or control (C). Data presented as the mean values extrapolated from **Table 3**. (a) Plot of average vessel length (μm). (b) Plot of average vessel number.
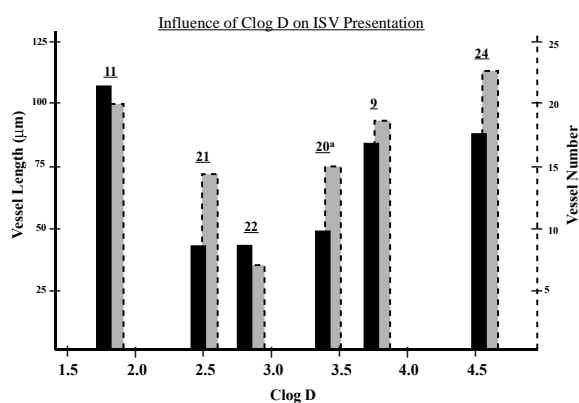[a] The data for compound **20** was obtained at 5μg/mL dosage.

Figure 9. Comparison of vessel length and vessel number to Clog D. The solid black bars correspond to vessel length and are plotted via the solid left axis. The associated vessel number is depicted by the dashed grey shaded bars and is plotted via the corresponding dashed right axis. Data extrapolated from **Table 3** and represetned as the mean values.
[a] The data for compound **20** was obtained at 5μg/mL dosage.

Figure 10. Dose-response behavior for selected phthalimidines **21** and **22**. Average vessel length and vessel number are expressed as mean values. Compounds and evaluated doses are represented by three-bar groupings as indicated in each plot.

When contemplating the anti-angiogenesis data in relation to the nitrite and TNF-α results, it is important to place in context the method of compound administration; with *in vitro* routes, compounds are applied directly to cells, while in the zebrafish embryo model, they are diluted into the tank water. The amount of analyte taken up by the zebrafish embryo is naturally variable, and the associated bioavailability is likely related to the polarity of the compounds in question. It is therefore also reasonable to hypothesize that for a supplied dosage, some phthalimidines are actually more anti-angiogenic than indicated; understandably, the *fli1*:EGFP assay simply may not translate such heightened effects for substrates of particular lipophilicity. It should be noted, however, that most of the compounds were generally well tolerated in RAW246.7 (see **Table 1**), suggesting that anti-angiogenic activity was likely attributable to selective targeting by our phthalimidines and not derivative of non-specific declines in protein synthesis consequent of drug-induced toxicity.

2.4 Hypothesis on Potential Mechanism of Action

Our preliminary investigations revealed novel adamantyl phthalimidines as molecules with desirable biological properties and possessing noteworthy anti-nitrite activity. Given that cellular nitrite is linked to nitric oxide production and the associated radical pathways,[20] we wondered if our molecules could act as radical scavengers, limiting nitrite by directly intercepting reactive oxygen (ROS) and nitrogen species (RNS). Horvat and colleagues[21] have reported the diradical character and reactivity of activated *N*-(1-adamantylmethyl) and *N*-(2-adamantylmethyl) phthalimides, and we realized the structural analogies inherent in our own system. We therefore hypothesized that adamantyl phthalimidines might possess two radical-active positions (**Scheme 4**). In the top pathway, radical excitation or enzymatic initiation is followed by carbon-carbon bond formation, eventually leading to complex ring-expanded products. The lower pathway highlights adamantyl-type capture of ROS; elimination from Intermediate A provides a high-energy olefin[22] capable of sequestering a variety of reactive species. Such intracellular neutralization of toxic free radicals is often neuroprotective, reducing CNS damage and lowering the risk of cancer and diseases caused by oxidative stress.
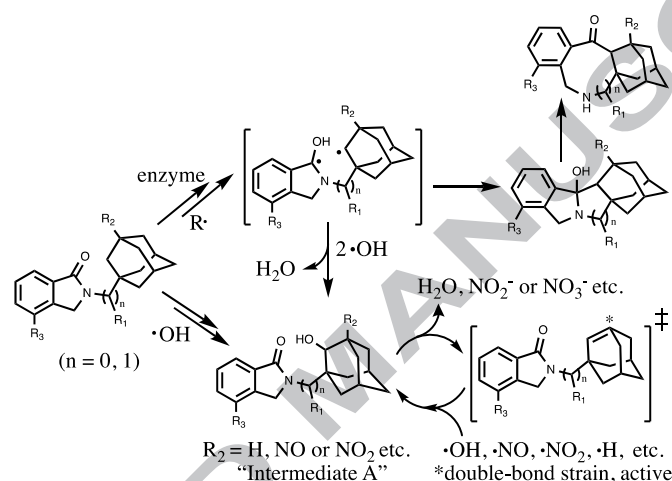
Scheme 4. A hypothetical model of adamantyl phthalimidines functioning as radical scavengers inside cells. The generic groups R_1, R_2 and R_3 are indicative of functional group locations and substitutent patterns characteristic to novel adamantyl phthalimidines.

3. Conclusion

Herein we have reported 15 new substituted adamantyl and noradamantyl phthalimidines that demonstrate desirable neuroprotective and anti-angiogenic properties. Through careful and thorough analysis of the associated nitrite and TNF-α data, we were able to discern various trends inherit to this focused library, subsequently establishing the framework for a primary structure activity relationship. In the logical progression, site-specific nitration, alkylation and thioamidation provided compound **24**, which when dosed at 30 μM, effected an 89% drop in LPS-induced nitrite production concurrent with only a 4% drop in TNF-α activity. Subsequent investigations revealed our novel phthalimidines as promising anti-angiogenics with **21** and **22**, in particular, demonstrating dose-response behavior on zebrafish vessel length at concentrations up to 50μg/mL. Collectively, these observations prompt further exploration into diversified phthalimidine architecture with the goals of enhancing the SAR, illuminating the underlying mechanisms of action and fostering amelioration of relevant biological activities.

4. Experimental

4.1 General methods for organic synthesis

Melting points (uncorrected) were measured with a Fisher-Johns apparatus. ^{1}H NMR, and ^{13}C NMR were recorded on a Bruker (Bellevica, MA) AC-300 spectrometer and a Varian AS400 spectrometer. MS (m/z) data were measured on an Agilent 5973 GC-MS (CI). Elemental analyses were performed by Atlantic Microlab, Inc.

For compounds **9**-**13**, a mixture of 77-155 mg (0.6-1.2 mmol) of phthaldialdehyde **8** and equal molar amount of appropriately substituted adamantylamine or noradamantylamine (if utilized as the hydrochloride salt, potassium carbonate, 0.55-1.0 eq, was added as appropriate) in 40-80 mL tetrahydrofuran was stirred for 171.5-211.0 h under a nitrogen atmosphere at room temperature. After removing solvent, the residues were purified by silica gel chromatography (EtOAc/Hex or MeOH/CH_2Cl_2).

For compounds, **16**-**22**, a mixture of 216-522 mg (0.8-1.9 mmol) of **15**, equal molar amount of potassium carbonate and equal molar amount of appropriately substituted adamantylamine or noradamantylamine (if utilized as the hydrochloride salt, potassium carbonate, 1.0-1.55eq, was added as appropriate) in 2-3 mL *N,N*-dimethylacetamide (DMA) was stirred for 18-71 h under a nitrogen atmosphere at room temperature, and then continuously reacted for 22-32 h at 50-58 ^{o}C. After removing solvent, the residues were purified by silica gel chromatography (EtOAc/Hex or MeOH/CH_2Cl_2) or by recrystallization with acetone.

For compounds **23**-**25**, A mixture of 45-100 mg (0.176-0.338 mmol) of appropriately substituted adamantylalkyl phthalimidine or noradamantyl phthalimidine and 0.55 to 1.0 molar ratio of Lawesson's reagent in 20 mL anhydrous toluene was refluxed for 15.5-22.0 h under a nitrogen atmosphere. After removing solvent, the residues were purified by silica gel chromatography (EtOAc/Hex).

*4.2. 2,3-Dihydro-2-[(tricyclo[3.3.1.1^{3,7}]dec-1-yl)methyl]-1H-isoindol-1-one (**9**)*

White solid (24%, from EtOAc/Hex); mp 148.0-149.0 ^{o}C ; ^{1}H NMR (CDCl$_3$) δ 7.85 (d, *J* = 7.3 Hz, 1H, C7-H), 7.55-7.41 (m, 3H, Ar-H), 4.50 (s, 2H, C3-H), 3.26 (s, 2H, NCH$_2$Ad), 1.99-1.57 (m, 15H, Ad-H) ppm; ^{13}C NMR (CDCl$_3$) δ 169.5, 141.4, 132.9, 131.1, 127.9, 123.8, 122.4, 55.8, 54.0, 41.1, 36.9, 36.0 and 28.4 ppm; MS (CI/CH$_4$), m/z 282 (MH$^+$); Anal. calcd for C$_{19}$H$_{23}$NO1/5H$_2$O: C, 80.07; H, 8.28; N, 4.91. Found: C, 80.08; H, 8.13; N, 4.70.

*4.3. 2,3-Dihydro-2-[1-(1-tricyclo[3.3.1.1^{3,7}]dec-1-yl)ethyl]-1H-isoindol-1-one (**10**)*

White needle crystals (60%, from EtOAc/Hex); mp 185.0-186.5 ^{o}C; ^{1}H NMR (DMSO-d_6) δ 7.68 (d, *J* = 7.4 Hz, 1H, C7-H), 7.62-7.45 (m, 3H, Ar-H), 4.54 (s, 2H, C3-H), 4.01 (q, *J* = 7.2 Hz, 1H, NCHMeAd), 1.98-1.41 (m, 15H, Ad-H) and 1.21 (d, *J* = 7.2 Hz, 3H, CH$_3$) ppm; ^{13}C NMR (DMSO-d_6) δ 168.2, 142.4, 132.6, 131.5, 128.2, 123.7, 123.2, 39.3, 37.4, 36.9, 28.3 and 12.6 ppm; MS (CI/CH$_4$), m/z 295 (M$^+$); Anal. calcd for C$_{20}$H$_{25}$NO: C, 81.31; H, 8.53; N, 4.74. Found: C, 81.01; H, 8.46; N, 4.62.

*4.4. 2,3-Dihydro-2-(3-hydroxy-tricyclo[3.3.1.1^{3,7}]dec-1-yl)-1H-isoindol-1-one (**11**)*

White crystals (41%, from MeOH/CH_2Cl_2); mp 218.5-219.5 ^{o}C; ^{1}H NMR (CDCl$_3$) δ 7.79 (d, *J* = 7.4 Hz, 1H, C7-H), 7.52-7.39 (m, 3H, Ar-H), 4.47 (s, 2H, C3-H), 3.48 (s, 1H, OH), 2.43-1.55 (m, 14H, Ad-H) ppm; ^{13}C NMR (CDCl$_3$) δ 168.9, 140.8, 134.3, 131.0, 127.9, 123.3, 122.4, 69.2, 57.8, 47.7, 44.1, 38.7, 34.9 and 30.8 ppm; MS (CI/CH$_4$), m/z 284 (MH$^+$); Anal. calcd for C$_{18}$H$_{21}$NO21/5H$_2$O: C, 75.34; H, 7.52; N, 4.88. Found: C, 75.38; H, 7.23; N, 4.75.

4.5. 2,3-Dihydro-2-(tricyclo[3.3.1.1^{3,7}]dec-2-yl)-1H-isoindol-1-one (**12**)

White needle crystals (62%, from MeOH/CH$_2$Cl$_2$); mp 121.5-123.0 ^{o}C; ^{1}H NMR (CDCl$_3$) δ 7.83 (d, J = 7.7 Hz, 1H, C7-H), 7.54-7.41 (m, 3H, Ar-H), 4.67 (s, 2H, C3-H), 4.34 (s, 1H, C2'-H) and 2.49-1.71 (m, 14H, Ad-H) ppm; ^{13}C NMR (CDCl$_3$) δ 169.3, 141.6, 133.0, 131.0, 127.8, 123.3, 122.4, 58.3, 50.3, 38.2, 37.8, 32.7, 31.7, 27.6 and 27.3 ppm; MS (CI/CH$_4$), m/z 267 (M$^+$); Anal. calcd for C$_{18}$H$_{21}$NO1/10H$_2$O: C, 80.32; H, 7.94; N, 5.20. Found: C, 80.06; H, 7.88; N, 5.03.

4.6. 2,3-Dihydro-2-(tricyclo[3.3.1.0^{3,7}]non-3-yl)-1H-isoindol-1-one (**13**)

White needle crystals (60%, from MeOH/CH$_2$Cl$_2$); mp 151.5-153.0 ^{o}C; ^{1}H NMR (CDCl$_3$) δ 7.82 (d, J = 6.9 Hz, 1H, C7-H), 7.50-7.41 (m, 3H, Ar-H), 4.50 (s, 2H, C3-H) and 2.99-1.55 (m, 13H, Norad-H) ppm; ^{13}C NMR (CDCl$_3$) δ 168.9, 141.2, 134.4, 130.8, 127.9, 123.1, 122.4, 67.8, 49.3, 47.6, 43.4, 42.3, 37.2 and 34.7 ppm; MS (CI/CH$_4$), m/z 253 (M$^+$); Anal. calcd for C$_{17}$H$_{19}$NO1/10H$_2$O: C, 80.03; H, 7.58; N, 5.49. Found: C, 79.99; H, 7.29; N, 5.41.

4.7. Methyl 2-bromomethyl-3-nitrobenzoate (**15**)

A mixture of 18.7 g (95.8 mmol) of methyl 2-methyl-3-nitrobenzoate **14**, 17.1 g (96.1 mmol) of *N*-bromosuccinimide and 0.7 g (2.9 mmol) of benzoyl peroxide in 500 mL carbon tetrachloride was refluxed for 20 h. The reaction mixture was cooled and concentrated. Thereafter, it was precipitated and washed by ethyl ether to afford product **15** (22.3 g, 84.8%) as yellowish crystals: mp 68.0-70.0 ^{o}C (ref. 67-70 ^{o}C). Prepared in accordance with reference 15 (Hay, J. V. *US* 4,678,500 A **1987**).

4.8. 2,3-Dihydro-4-nitro-2-(tricyclo[3.3.1.1^{3,7}]dec-1-yl)-1H-isoindol-1-one (**16**)

Yellowish solid (54%, from EtOAc/Hex); mp 214.0-215.5 ^{o}C; ^{1}H NMR (CDCl$_3$) δ 8.37 (d, J = 7.6 Hz, 1H, C7-H), 8.12 (d, J = 7.6 Hz, 1H, C5-H), 7.66 (t, J = 7.6 Hz, 1H, C6-H), 4.93 (s, 2H, C3-H) and 2.43-1.73 (m, 15H, Ad-H) ppm; ^{13}C NMR (CDCl$_3$) δ 166.1, 143.2, 138.0, 136.5, 129.6, 129.4, 126.2, 56.2, 48.6, 40.0, 36.4, 36.2, 29.7 and 29.6 ppm; MS (CI/CH$_4$), m/z 312 (M$^+$); Anal. calcd for C$_{18}$H$_{20}$N$_2$O$_3$1/2H$_2$O: C, 67.27; H, 6.59; N, 8.72. Found: C, 67.18; H, 6.36; N, 8.55.

4.9. 2,3-Dihydro-4-nitro-2-[(tricyclo[3.3.1.1^{3,7}]dec-1-yl)methyl]-1H-isoindol-1-one (**17**)

White crystals (63%, from MeOH/CH$_2$Cl$_2$); mp 178.5-179.5 ^{o}C; ^{1}H NMR (CDCl$_3$) δ 8.35 (d, J = 7.6 Hz, 1H, C7-H), 8.11 (d, J = 7.6 Hz, 1H, C5-H), 7.65 (t, d, J = 7.6 Hz, 1H, C6-H), 4.92 (s, 2H, C3-H), 3.26 (s, 2H, NCH$_2$Ad) and 2.04-1.47 (m, 15H, Ad-H) ppm; ^{13}C NMR (CDCl$_3$) δ 167.0, 143.2, 137.0, 136.1, 129.9, 129.6, 126.5, 55.9, 54.8, 41.1, 36.8, 36.0, 28.4 and 28.3 ppm; MS (CI/CH$_4$), m/z 326 (M$^+$); Anal. calcd for C$_{19}$H$_{22}$N$_2$O$_3$1/2H$_2$O: C, 68.04; H, 6.91; N, 8.35. Found: C, 68.10; H, 6.72; N, 8.15.

4.10. 2,3-Dihydro-4-nitro-2-[1-(1-tricyclo[3.3.1.1^{3,7}]dec-1-yl)ethyl]-1H-isoindol-1-one (**18**)

Yellow crystals (42%, by recrystallization with acetone); mp 187.5-188.5 ^{o}C; ^{1}H NMR (DMSO-d_6) δ 8.40 (d, J = 7.6 Hz, 1H, C7-H), 8.11 (d, J = 7.6 Hz, 1H, C5-H), 7.78 (t, J = 7.6 Hz, 1H, C6-H), 4.91 (s, 2H, C3-H), 3.99 (q, J = 7.3 Hz, 1H, NCHMeAd), 1.91-1.41 (m, 15H, Ad-H) and 1.21 (d, J = 7.3 Hz, 3H, CH$_3$) ppm; ^{13}C NMR (DMSO-d_6) δ 166.2, 143.7, 138.0, 135.8, 130.3, 129.8, 126.8, 39.3, 37.6, 36.8, 28.4, 28.3, 28.2 and 12.5 ppm; MS (CI/CH$_4$), m/z 340 (M$^+$); Anal. calcd for C$_{20}$H$_{24}$N$_2$O$_3$: C, 70.56; H, 7.11; N, 8.23. Found: C, 70.28; H, 6.97; N, 8.15.

*4.11. 2,3-Dihydro-4-nitro-2-(3-hydroxy-tricyclo[3.3.1.1^{3,7}]dec-1-yl)-1H-isoindol-1-one (**19**)*

White crystals (45%, from MeOH/CH$_2$Cl$_2$); mp 230.0-231.5 ^{o}C; ^{1}H NMR (DMSO-d_6) δ 8.37 (d, J = 7.9 Hz, 1H, C7-H), 8.02 (d, J = 7.9 Hz, 1H, C5-H), 7.75 (t, J = 7.9 Hz, 1H, C6-H), 4.96 (s, 2H, C3-H), 4.61 (s, 1H, OH) and 2.19-1.46 (m, 14H, Ad-H) ppm; ^{13}C NMR (DMSO-d_6) δ 165.7, 143.4, 137.4, 137.3, 130.3, 129.5, 126.8, 67.9, 58.0, 48.8, 47.5, 44.3, 38.3, 35.0 and 30.6 ppm; MS (CI/CH$_4$), m/z 328 (M$^+$); Anal. calcd for C$_{18}$H$_{20}$N$_2$O$_4$: C, 65.84; H, 6.14; N, 8.53. Found: C, 65.48; H, 6.09; N, 8.34.

*4.12. 2,3-Dihydro-4-nitro-2-(tricyclo[3.3.1.1^{3,7}]dec-2-yl)-1H-isoindol-1-one (**20**)*

Yellowish crystals (48%, from MeOH/CH$_2$Cl$_2$); mp 179.0-180.5 ^{o}C; ^{1}H NMR (Acetone-d_6) δ 8.44 (d, J = 7.5 Hz, 1H, C7-H), 8.12 (d, J = 7.5 Hz, 1H, C-5H), 7.85 (t, J = 7.5 Hz, 1H, C6-H), 5.21 (s, 2H, C3-H), 4.29 (s, 1H, C2'-H) and 2.51-1.76 (m, 14H, Ad-H) ppm; ^{13}C NMR (Acetone-d_6) δ 166.3, 143.6, 137.7, 136.4, 129.6, 129.1, 126.2, 59.0, 50.7, 37.9, 37.5, 32.3, 31.3, 27.6 and 27.2 ppm; MS (CI/CH$_4$), m/z 312 (M$^+$); Anal. calcd for C$_{18}$H$_{20}$N$_2$O$_3$: C, 69.21; H, 6.45; N, 8.97. Found: C, 69.07; H, 6.51; N, 8.79.

*4.13. 2,3-Dihydro-4-amino-2-(tricyclo[3.3.1.1^{3,7}]dec-2-yl)-1H-isoindol-1-one (**21**)*

A mixture of 60.0 mg (0.192 mmol) of 2,3-dihydro-4-nitro-2-(tricyclo[3.3.1.1^{3,7}]dec-2-yl)-1*H*-isoindol-1-one **20** and 104 mg of palladium on carbon (10 wt.%) in 100 mL methanol was shaken for 67 h under the hydrogen atmosphere (46 lbs.) at room temperature. Thereafter, filtrate was chromatographed on silica gel (MeOH/CH$_2$Cl$_2$ = 1/20) to provide product **21** as a gum (28.8 mg, 53.1%): ^{1}H NMR (CDCl$_3$) δ 7.31-7.25 (m, 2H, C7, C6-H), 6.82 (d, J = 8.4 Hz, 1H, C5-H), 4.52 (s, 2H, C3-H), 4.34 (s, 1H, C2'-H), 3.80 (s, br, 2H, NH$_2$) and 2.36-1.72 (m, 14H, Ad-H) ppm; ^{13}C NMR (CDCl$_3$) δ 169.8, 140.6, 133.9, 129.2, 126.6, 117.4, 114.0, 58.3, 48.1, 38.3, 37.8, 32.8, 31.8, 27.6 and 27.3 ppm; MS (CI/CH$_4$), m/z 282 (M$^+$).

*4.14. 2,3-Dihydro-4-nitro-2-(tricyclo[3.3.1.0^{3,7}]non-3-yl)-1H-isoindol-1-one (**22**)*

White crystals (70%, from MeOH/CH$_2$Cl$_2$); mp 216.0-217.5 ^{o}C; ^{1}H NMR (CDCl$_3$) δ 8.35 (d, J = 7.8 Hz, 1H, C7-H), 8.12 (d, J = 7.8 Hz, 1H, C5-H), 7.66 (t, J = 7.8 Hz, 1H, C6-H), 4.94 (s, 2H, C3-H) and 3.04-1.57 (m, 13H, Norad-H) ppm; ^{13}C NMR (CDCl$_3$) δ 166.0, 143.3, 137.7, 136.8, 129.5, 129.4, 126.2, 68.2, 50.3, 47.6, 43.4, 42.3, 37.1 and 34.6 ppm; MS (CI/CH$_4$), m/z 298 (M$^+$); Anal. calcd for C$_{17}$H$_{18}$N$_2$O$_3$1/3H$_2$O: C, 67.09; H, 6.18; N, 9.20. Found: C, 66.97; H, 5.96; N, 9.07.

*4.15. 2,3-Dihydro-2-[1-(1-tricyclo[3.3.1.1^{3,7}]dec-1-yl)ethyl]-1H-isoindol-1-thione (**23**)*

Yellow solid (57%); mp 199.0-200.5 ^{o}C; ^{1}H NMR (DMSO-d_6) δ 7.85 (d, J = 7.6 Hz, 1H, C7-H), 7.61-7.47 (m, 3H, Ar-H), 5.06 (q, J = 7.1 Hz, 1H, NCHMeAd), 4.86 (s, 2H, C3-H), 1.97-1.47 (m, 15H, Ad-H) and 1.21 (d, J = 7.1 Hz, 3H, CH$_3$) ppm; ^{13}C NMR (DMSO-d_6) δ 192.9, 141.1, 139.4, 131.7, 128.4, 125.5, 123.0, 59.7, 55.5, 39.3, 37.7, 36.8, 28.4 and 12.8 ppm; MS (CI/CH$_4$), m/z 309 (M-2); Anal. calcd for C$_{20}$H$_{25}$NS: C, 77.12; H, 8.09; N, 4.50. Found: C, 76.83; H, 8.03; N, 4.38.

*4.16. 2,3-Dihydro-4-nitro-2-[1-(1-tricyclo[3.3.1.1^{3,7}]dec-1-yl)ethyl]-1H-isoindol-1-thione (**24**)*

Orange-red crystals (46%); mp 211.5-212.5 ^{o}C; ^{1}H NMR (CDCl$_3$) δ 8.49-8.36 (m, 2H, C5, C7-H), 7.69 (t, J = 8.7 Hz, 1H, C6-H), 5.29-5.09 (m, 3H, C3-H, NCHMeAd), 2.09-1.61 (m, 15H, Ad-H) and 1.35 (d, J = 8.1 Hz, 3H, CH$_3$) ppm; ^{13}C NMR (CDCl$_3$) δ 191.3, 143.0, 142.4, 135.1, 132.6, 129.7, 126.1, 60.4, 56.6, 39.7, 38.2, 36.8, 28.4 and 12.7 ppm; MS (CI/CH$_4$), m/z 356 (M$^+$); Anal. calcd for C$_{20}$H$_{24}$N$_2$O$_2$S1/5H$_2$O: C, 66.71; H, 6.83; N, 7.78. Found: C, 66.38; H, 6.53; N, 7.40.

*4.17. 2,3-Dihydro-2-(tricyclo[3.3.1.0^{3,7}]non-3-yl)-1H-isoindol-1-thione (**25**)*

Yellowish needle crystals (72%); mp 185.0-186.5 °C; ^{1}H NMR (DMSO-d$_6$) δ 7.84 (d, *J* = 7.7 Hz, 1H, C7-H), 7.58-7.47 (m, 3H, Ar-H), 4.99 (s, 2H, C3-H) and 2.61-1.53 (m, 13H, Norad-H) ppm; ^{13}C NMR (DMSO-d$_6$) δ 190.9, 141.6, 140.4, 131.4, 128.3, 124.5, 122.6, 72.3, 58.0, 46.4, 43.3, 40.9, 37.0 and 34.8 ppm; MS (CI/CH$_4$), m/z 267 (M-2); Anal. calcd for C$_{17}$H$_{19}$NS: C, 75.79; H, 7.11; N, 5.20. Found: C, 75.68; H, 6.96; N, 5.14.

5. Biological assays

5.1. Assessments of drug anti-TNF-α and anti-nitric oxide generation in RAW 264.7 cells

RAW 264.7 cells were purchased from ATCC (Manassas, VA, USA). The cells were grown in DMEM media (Invitrogen, DMEM, high glucose, GlutaMAX™ Supplement, pyruvate, #10569-010) supplemented with 10% FBS (Invitrogen, Fetal Bovine Serum, qualified, heat inactivated, #16140-071) with penicillin and streptomycin (Invitrogen, Penicillin-Streptomycin (10,000 U/mL), #15140-122) and were maintained at 37 °C and 5% CO$_2$. The cells were grown to 75% to 85 % confluence on 10 cm plates (Corning-Falcon, #353003) following the protocol described by ATCC. To assess for drug effects on LPS-induced markers of inflammation, namely TNF-α protein and nitrite ion levels (NO$_2^-$, a stable end-product of nitric oxide metabolism) cells were seeded into 24 well plates (VWR, #10062-896) at a density of 200 x 10^3 cells per well. On each plate there was one blank well where no cells were added yet culture media in the well was treated similarly to wells with cells (n=1). The blank well media was used for background subtractions for various downstream assays. Twenty-four hours after seeding the plate the seeding media was replaced with fresh media. Two hours after this the cells were exposed to a range of concentrations of drug test-compound(s) dissolved in 100% tissue culture grade dimethyl sulfoxide (DMSO, SIGMA #D2650). Drug stocks were prepared in a 200 times more concentrated stock in DMSO. The final concentration of DMSO added to the cells was 0.5%. The effects of each concentration of drug were assessed in 4 wells per concentration in the 24 well plate (n=3$^\#$-4). On each plate one set of wells were assigned as drug-vehicle controls (i.e. DMSO), one test compound was assessed on one 24 well plate. The drug concentrations used for each test agent were 1, 10 and 30 μM and are indicated in the associated figures. One hour after the drugs were added the cells were challenged with lipopolysaccharide (LPS, SIGMA, serotype 055:B5) at a final concentration of 60 ng/ml. Twenty to twenty-four hours after the cells were challenged with LPS the culture media was collected and utilized for the measurement of markers of inflammation.

5.2. Enzyme-Linked Immunosorbent Assay for TNF-α protein

Media TNF-α levels were measured by use of the BioLegend ELISA MAX™ Set Delux ELISA (#430904). The protocol used was that recommended by the manufacturer. In brief a day prior to performing the assay a 96 well plate was coated with a capture antibody directed against TNF-α. The following day the assay plate was washed and blocked with the kit blocking agent for 1 hour while being mixed on a plate shaker at 200 rpm (all incubations were mixed at 200 rpm unless stated otherwise). A TNF-α protein standard curve was prepared in the assay diluent following the kit instructions and unknown media samples were likewise diluted in the same assay diluent. After blocking, the plate was washed and then both the standards and unknown media samples were added to the plate in duplicate. The standards and unknown samples were incubated for 2 hours. After the incubation the plate was washed and then the biotin labeled detection antibody was added to each well and incubated for a further 1 hour. After this incubation the avidin-HRP conjugate complex was added to each well and incubated for 30 min. The plate was washed and the chromogenic substrate 3,3',5,5'-tetramethylbenzidine solution was added to each well. At this point the plate was covered and incubated in the dark for 15 minutes, with no mixing. After 15 minutes the chromogenic reaction was stopped by the addition of 2N H$_2$SO$_4$ and the absorbance was read at 450 nm and for background subtractions at 570 nm, on a SPECTRAmax PLUS plate reader. The absorbances were used to generate a TNF-α protein standard curve and the protein levels in the unknown samples were determined using SoftMax Pro V5, Molecular Devices.

5.3. Nitrite ion detection in drug treated RAW 267.4 cell culture media

To measure the levels of nitrite ion (NO_2^-) we utilized the Griess Reagent System (Promega, Madison, WI, Cat # G2930). The protocol followed was that recommended by the manufacturer, in brief a NO_2^- ion standard curve was prepared in culture media of the same composition to that used for the cell culture study. The concentration range of the standard curve was from 1.5 µM to 100 µM. Equal volumes (50 µl) of standards and unknown samples were added to clear 96 well plates in duplicate. Then 50 µl of sulfanilamide solution was added to each well and the plate was covered and incubated in the dark for 10 minutes. After the incubation period 50 µl of N-1-napthylethylenediamine dihydrochloride solution was added to each well and the plate was incubated in the dark for a further 10 minutes. After this incubation the plate was read at 550 nm on a SPECTRAmax PLUS plate reader and the absorbances were used to generate a NO_2^- standard curve and the NO_2^- ion levels of the unknown samples are determined using SoftMax Pro V5, Molecular Devices.

5.4. Cellular viability assessment of drug treated RAW 264.7 cells

RAW 264.7 cell viability was determined by use of the CellTiter 96 AQueous One Solution Cell Proliferation Assay (Promega, Madison, WI). Changes in cellular health status were determined by use of indirect measures related to the formation of a colored tetrazolium dye product that can be measured spectrophotometrically at 490 nm. An increase in absorbance at 490 nm is indicative of an increase in numbers of healthy cells, similarly a reduction in absorbance is indicative of a reduction of healthy cells. After the culture media was harvested for use in TNF-α and NO_2^- ion assays, the media was replaced with 0.5 ml of fresh media plus 100 µl of the cell viability reaction mixture. After a 20 to 30 minute incubation at 37 ^{o}C with 5% CO_2 the absorbance at 490 nm was obtained using an infinite M200 PRO plate reader (TECAN, USA).

5.5. Statistical Analyses for RAW-derived assays

Data are expressed as a percentage change from the DMSO-vehicle control measurements. Measurements are expressed as mean ± standard errors, where the n number represents the number of wells in a 24 well plate. Due to the presence of one blank control well on each plate, for some drug concentrations the n number is 3[#] and not 4. Statistical comparisons were undertaken by use of a One-Way ANOVA with appropriate Bonferroni corrections for multiple comparisons, as required (GraphPad InStat Version 3.05). P values of <0.05 are considered to be of statistical significance.

5.6. Zebrafish anti-angiogenesis assays

Zebrafish experiments were performed as previously described in references 13a-b (Beedie *et al*., **2016**, Mahony *et al*., **2013**) and references 17a-c (Beedie *et al*., **2015,** Therapontos *et al.,* **2009**, Beedie *et al*., **2017**.) Briefly, *fli1*:EGFP zebrafish (Zebrafish International Resource Centre, Oregon, USA) were maintained in aquarium housing at 28°C. Zebrafish pairs were mated and embryos were collected. Lines transgenic for GFP were identified using a fluorescent microscope. At 24 hours post fertilization, embryos were manually dechorionated and the zebrafish moved to plates containing the compounds to be tested. Zebrafish were exposed to each compound for 24 hours, at which point they were anaesthetized with 0.1% tricaine. Microscopic imaging under blue fluorescent light was then used to assess vessel development. ImageJ was used to quantify vessel length and number excluding the posterior 5 intersegmental vessels. All animal work was licensed and carried out in accordance with UK Home office and institutional ethical and welfare guidelines.

Competing Interests

Authors NG, NV, WDF, DT, SB and WL have patents on these compounds. US patent application No. US2016/054430.

Supplementary Data

Supplementary data associated with this article can be found, in the online version, at

References

[1] (a) For a recent review on redox signaling and oxidative stress, see: Schieber, M.; Chandel, N. S. *Current Biology* **2014**, *24*, R453-R462. (b) Shahani, N.; Sawa, A. *Antioxid. Redox Signal.* **2011**, *14(8)*, 1493. (c) Chung, K. K.; David, K. K. *Nitric Oxide* **2010**, *22(4)*, 290.

[2] (a) Moncada, S.; Palmer, R. M. J.; Higgs, E. A. *Biochemical Pharmacology* **1989**, *38(11)*, 1709. (b) Aldskogius, H.; Liu, L.; Syensson, M. *J. Neurosci. Res.* **1999**, *58*, 33.

[3] (a) Saxena S.; Caroni P. *Neuron* **2001**, *71*, 35. (b) Bredesen D. E. *Mol Neurodegener.* **2009**, 4:27.

[4] (a) Swardfager, W.; Lanctot, K.; Rothenburg, L.; Wong, A.; Cappell, J.; Herrmann, N. *Biol Psychiatry* **2010**, *68(10)*, 930. (b) Locksley, RM.; Killeen, N.; Lenardo, MJ. *Cell* **2001**, *104(4)*, 487. (c) Dowlati, Y.; Herrmann, N.; Swardfager, W.; Liu, H.; Sham, L.; Reim, EK. *Biol Psychiatry* **2010**, *67(5)*, 446. (d) Brynskov, J.; Foegh, P.; Pedersen, G.; Ellervik, C.; Kirkegaard, T.; Bingham, A. *Gut* **2002**, *51(1)*, 37. (e) Frankola, K. A.; Greig, N. H.; Luo, W.; Tweedie, D. *CNS & Neurological Disorders - Drug Targets* **2011**, *10,* 391. (f) Tweedie, D.; Luo, W; Short, R. G.; Brossi, A.; Holloway, H. W.; Li, Y.; Yu, Q.; Greig, N. H. *J. Neumeth.* **2009**, *183*, 182. (g) Carmeliet, P.; Jain, R. K. *Nature* **2000**, 407, 249. (h) Coussens, L. M.; Werb, Z. *Nature* **2002**, 420, 860. (i) Balkwill, F.; Coussens, L. M. *Nature* **2004**, 431, 405.

[5] Tarkowski E.; Blennow, K.; Wallin, A.; Tarkowski, A. *J. Clin. Immunol.* **1999**, *19,* 223.

[6] Tarkowski, E.; Andreasen, N.; Tarkowski, A.; Blennow, K. *J. Neurol. Neurosurg. Psychiatry* **2003**, *74*, 1200.

[7] (a) Ohkuma, S.; Katsura, M. *Progress in Neurobiology* **2001**, *64*, 97. (b) Bloodsworth, A.; O'Donnell, V. B.; Freeman, B. A. *Arterioscler Thromb Vasc Biol* **2000**, *20*, 1707.

[8] (a) Knowles, R. G.; Palacios, M.; Palmer, R. M.; Moncada, S. *Proc Natl Acad Sci USA* **1989**, *86*, 5119. (b) Snyder, S. H.; Bredt, D. S. *Trends Pharmacol Sci* **1991**, *12*, 125. (c) Law, A.; Gauthier, S.; Quirion, R. *Brain Research Reviews* **2001**, *35*, 73. (d) Hoffman, M. A. *Science* **1991**, *252*, 1788. (e) Lancaster, F. E. *Alcohol Clin Exp Res* **1992**, *16,* 539. (f) Nowicki, J. P.; Duval, D.; Poignet, H.; Scatton, B. *Eur J Pharmacol* **1991**, *204*, 339. (g) Eliasson, M. J.; Huang, Z.; Ferrante, R. J.; Sasamata, M.; Molliver, M. E.; Snyder, S. H.; Moskowitz, M. A. *J. Neurosci* **1999**, *19*, 5910.

[9] Goodwin, J. L.; Uemura, E.; Cunnick, J. E. *Brain Research* **1995** *692*, 207.

[10] Jenkins, D. C.; Charles, I. G.; Thomsen, L. L.; Moss, D. W.; Homes, L. S.; Baylis, S. A.; Rhodes, P.; Westmore, K.; Emson, P. C.; Moncada, S. *Proc. Natl. Acad. Sci. USA* **1995**, *92,* 4392.

[11] Greig, N. H.; Luo, W.; Tweedie, D.; Holloway, H. W.; Yu, Q.; Goetzl, E. J. *US 8,927,725 B2* **2015**.

[12] (a) Petit, A.; Bihel, F.; Costa, C. A.; Pourquié, O.; Checler, F.; Kraus, J. *Nature cell Biology* **2001**, *3*, 507. (b) Christie, G.; Markwell, R. E.; Gray, C. W.; Smith, L.; Godfrey, F.; Mansfield, F.; Wadsworth, H.; King, R.; McLaughlin, M.; Cooper, D. G.; Ward, R. V.; Howlett, D. R.; Hartmann, T.; Lichtenthaler, S. F.; Beyreuther, K.; Underwood, J.; Gribble, S. K.; Cappai, R.; Masters, C. L.; Tamaoka, A.; Gardner, R. L.; Rivett, A. J.; Karran, E. H. Allsop, D. *J. Neurochem.* **1999**, *73,* 195. (c) Citron, M.; Diehl, T. S.; Capell, A.; Haass, C.; Teplow, D. B.; Selkoe, D. J. *Neuron*, **1996**, *17*, 171. (d) Joubert, J.; Dyk, S.; Green, I. R.; Malan, S. F. *Bioorg. Med. Chem.* **2011**, *19*, 3935. (e) Mizoguchi, K.; Yokoo, H.; Yoshida,M.; Tanaka, T.; Tanaka, M. *Brain Research* **1994**, *662*, 255. (f) Danysz, W.; Parsons, C. G.; Kornhuber, J.; Schmidt, W. J.; Quack, G. *Neuroscience and Biobehavioral Reviews* **1997**, *21(4)*, 455. (g) Parsons, C. G.; Danysz, W.; Quack, G. *Neuropharmacology* **1999**, *38*, 735. (h) Zou, J. Y.; Crews, F. T. *Brain Research* **2005**, *1034*, 11. (i) Joubert, J.; Dyk, S.; Malan, S. F. *Bioorg. Med. Chem.* **2008**, *16*, 8952. (j) Neuraxon Inc. *WO20007118314*, **2007**.

[13] (a) Paci, C.; Thomas, A.; Onofrj, M. *Nerol Sci* **2001**, *22*, 75. (b) Pinna, A.; Chiara, G. D.; Wardas, J.; Morelli, M. *Eur. J. Neurosci.* **1996**, *8*, 1176. (c) Ferré, S.; O'Connor, W. T.; Fuxe, K.; Ungerstedt, U. *The Journal of Neuroscience* **1993**, *13(12),* 5402. (d) Baldessarini, R. J.; Lipinski, J. F. Chace, K. V. *Biochemical Pharmacology* **1972**, *21*, 77. (e) Merello, M.; Nouzeilles, M. I.; Cammarota, A.; Leiguarda, R. *Clinical Neuropharmacology* **1999**, 22(5), 273. (f) Standaert, D. G.; Young, A. B. " The Pharmacological Basis of Therapeutics " McGraw-Hill, New York, **2001**, pp. 549. (g) Moryl, E.; Danysz, W.; Quack, G. *Pharmacology & Toxicology* **1993**, *72*, 394.

[14] (a) Beedie, S. L.; Rore, H. M.; Barnett, S.; Chau, C. H.; Luo, W.; Greig, N. H.; Figg, W. D.; Vargesson, N. *Oncotarget*, **2016**, *7(22)*, 33237. (b) Mahony, C.; Erskine, L.; Niven, J.; Greig, N. H.; Figg, W. D.; Vargesson, N. *Proc. Natl. Acad. Sci. USA* **2013**, *110*, 12703. (c) Horvat, M.; Uzelac, L.; Marjanovic, M; Cindro, N.; Frankovic, O.; Mlinaric-Majerski, K.; Kralj, M.; Basaric, N. *Chem. Biol. Drug Des.* **2012**, *79*, 497. (d) Aragon-Ching, J. B.; Li, H.; Gardner, E. R.; Figg, W. D. *Recent Pat. Anticancer Drug Discov.* **2007**, *2*, 167.

[15] Mateo, A; Pilar, S; Carmen, L; Angel, A. *J. Org. Chem.* **2005**, *70*, 7617.

[16] Hay, J. V. *US* 4,678,500 A **1987**

[17] Tweedie, D.; Frankola, K. A.; Luo, W.; Li, Y.; Greig, N. H. *The Open Biochemistry Journal*, **2011**, *5*, 37.

[18] We have previously studied the effects of known TNF-α inhibitor Lenalidomide, a phthalimidine-based analog of Thalidomide that is marketed under the name Revlimid. Under similar assay conditions to those detailed in this manuscript, Lenalidomide demonstrates TNF activity at 109% $\pm$ 10 of the control while maintaining cell viability of 106% $\pm$ 3. The primary experiments and data can be accessed in: Luo, W.; Yu, Q.; Salcedo, I.; Holloway, H. W.; Lahiri, D. K.; Brossi, A.; Tweedie, D.; Greig, N. H. *Bioorg. Med. Chem.* **2011**, *19*, 3965.

[19] (a) Beedie, S. L.; Peer, C. J.; Pisle, S.; Gardner, E. R.; Mahony, C.; Barnett, S.; Ambrozak, A.; Gutschow, M.; Chau, C. H.; Vargesson, N.; Figg, W. D. *Mol. Cancer Ther.* **2015**, *14*, 2228. (b) Therapontos, C.; Erskine, L.; Gardner, E. R.; Figg, W. D.; Vargesson, N. *Proc. Natl. Acad. Sci. USA.* **2009**, *106*, 8573. (c) Beedie, S. L.; Diamond, A. J.; Fraga, L. R.; Figg, W. D.; Vargesson, N. *Reprod. Toxicol.* **2017**, *70*, 49. (d) Lawson, N. D.; Weinstein, B. M. *Developmental Biology* **2002**, *248*, 307. (e) Chimote, G.; Sreenivasan, J.; Pawar, N.; Subramanian, J.; Sivaramakrishnan, H.; Sharma, S. *Drug Des. Devel. Ther.* **2014**, *8*, 1107. (f) Serbedzija, G. N.; Flynn, E.; Willet, C. E. *Angiogenesis* **1999**, *3*, 353.

[20] Snyder, S. H.; Bredt, D. S. *Sci Am* **1992**, 68.

[21] Horvat, M.; Görner, H.; Warzecha, K.; Neudörfl, J.; Griesbeck, A. G.; Mlinaric-Majerski, K.; Basaric, N. *J. Org. Chem.* **2009**, *74*. 8219.

[22] Bagrii, E. I.; Saginaev, A. T. *Russ. Chem. Rev.* **1983**, *52*, 1538.
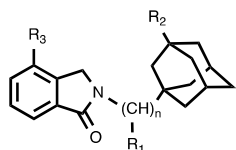
9 n = 1, $R_1 = R_2 = R_3 = H$
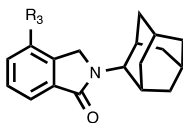**10** n = 1, $R_1 = CH_3, R_2 = R_3 = H$
11 n = 0, $R_1 = R_3 = H, R_2 = OH$

16 n = 0, $R_1 = R_2 = H, R_3 = NO_2$
17 n = 1, $R_1 = R_2 = H, R_3 = NO_2$
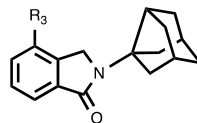**18** n = 1, $R_1 = CH_3, R_2 = H, R_3 = NO_2$
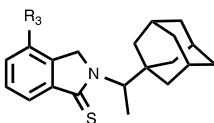**19** n = 0, $R_1 = H, R_2 = OH, R_3 = NO_2$

12 $R_3 = H$
20 $R_3 = NO_2$
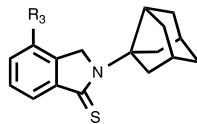**21** $R_3 = NH_2$

13 $R_3 = H$
22 $R_3 = NO_2$

23 $R_3 = H$
24 $R_3 = NO_2$

25 $R_3 = H$

N-adamantyl, substituted adamantyl and *N*-noradamantyl phthalimidines